RESEARCH ARTICLE

Sp100 Provides Intrinsic Immunity against Human Papillomavirus Infection

Wesley H. Stepp,[a,b] Jordan M. Meyers,[a]* Alison A. McBride[a]

Laboratory of Viral Diseases, NIAID, NIH, Bethesda, Maryland, USA[a]; Department of Microbiology and Immunology, Georgetown University School of Medicine, Washington, DC, USA[b]

* Present address: Jordan M. Meyers, Division of Infectious Diseases, Brigham and Women's Hospital, Harvard Medical School, Boston, Massachusetts, USA.

ABSTRACT **Most DNA viruses associate with, and reorganize, nuclear domain 10 (ND10) bodies upon entry into the host nucleus. In this study, we examine the roles of the ND10 components PML, Sp100, and Daxx in the establishment of human papillomavirus type 18 (HPV18) infection of primary human keratinocytes. HPV18 DNA or HPV18 quasivirus was introduced into primary human keratinocytes depleted of each ND10 protein by small interfering RNA technology, and genome establishment was determined by using a quantitative immortalization assay and measurements of viral transcription and DNA replication. Keratinocyte depletion of Sp100 resulted in a substantial increase in the number of HPV18-immortalized colonies and a corresponding increase in viral transcription and DNA replication. However, Sp100 repressed viral transcription and replication only during the initial stages of viral establishment, suggesting that Sp100 acts as a repressor of incoming HPV DNA.**

IMPORTANCE **The intrinsic immune system provides a first-line defense against invading pathogens. Host cells contain nuclear bodies (ND10) that are important for antiviral defense, yet many DNA viruses localize here upon cell entry. However, viruses also disrupt, reorganize, and modify individual components of the bodies. In this study, we show that one of the ND10 components, Sp100, limits the infection of human skin cells by human papillomavirus (HPV). HPVs are important pathogens that cause many types of infection of the cutaneous and mucosal epithelium and are the causative agents of several human cancers. Understanding how host cells counteract HPV infection could provide insight into antimicrobial therapies that could limit initial infection.**

Received 7 October 2013 **Accepted** 10 October 2013 **Published** 5 November 2013

Citation Stepp WH, Meyers JM, McBride AA. 2013. Sp100 provides intrinsic immunity against human papillomavirus infection. mBio 4(6):e00845-13. doi:10.1128/mBio.00845-13.

Editor Michael Imperiale, University of Michigan

Address correspondence to Alison A. McBride, amcbride@nih.gov.

Papillomaviruses are small DNA viruses that infect basal keratinocytes of the cutaneous and mucosal epithelia with striking host specificity. They cause both benign and malignant lesions and are the etiological sources of cervical malignancies in women (1). The small, circular genomes of human papillomaviruses (HPVs) are packaged in host histones into viral particles composed of a major and a minor capsid protein (L1 and L2, respectively).

Papillomaviruses establish their genomes as extrachromosomal replicons in host cell nuclei to create a stable, persistent infection. However, cells use countermeasures to sequester, disable, or eliminate incoming viral DNA to prevent it from establishing a transcriptional and replicative program (reviewed in reference 2). Interferon (IFN) production and induction of IFN-stimulated genes are some of the first responses of the innate immune system and help infected and neighboring cells combat viral infection (reviewed in reference 3). Nuclear domain 10 (ND10) bodies are IFN-responsive nuclear structures that play an important role in the intrinsic defense against viral infection (4, 5). They are composed of several constitutively expressed proteins that assemble into punctate nuclear foci (6, 7). The promyelocytic leukemia (PML) protein forms the structural scaffold of the ND10 body (8), and two transcriptional repressors, Sp100 and hDaxx, are highly enriched within the structures (reviewed in reference 9).

Studies of many DNA viruses indicate that ND10 bodies "sense" viral DNA and attempt to silence its gene expression as a first-line defense against viral infection (reviewed in reference 2). Counterintuitively, many virus genomes also localize to ND10 upon infection, where they initiate viral transcription and replication. However, many nucleus-resident DNA viruses have devised means to usurp this intrinsic defense and reorganize, modify, or disperse ND10 components. For example, the immediate-early gene product ICP0 of herpes simplex virus type 1 (HSV-1) degrades PML (10), which results in a more efficient viral infection. Similarly, another herpesvirus, human cytomegalovirus (HCMV), degrades Sp100 (11, 12) and Daxx (13–15) to enhance the early stages of infection. Moreover, RNA interference-mediated depletion of specific ND10 proteins results in enhanced early phases of infection of HSV-1 (16), varicella-zoster virus (VZV) (17), HCMV (18), and adenovirus type 5 (19). Thus, the components of ND10 bodies combat viruses at the first stages of viral infection, well before the slower innate and adaptive immune responses.

In contrast to some of the viruses described above, efficient

infection of papillomaviruses requires the presence of PML protein (20). Day et al. demonstrated that the transcription of bovine papillomavirus type 1 (BPV1) from both virions and reporter pseudovirus was much less efficient in PML$^{-/-}$ murine fibroblasts. An earlier study by the same group had shown that L2, the minor capsid protein of BPV1, localized to ND10 bodies and recruited both the viral genome and the viral transcription/replication protein E2 to this location (21). Initially, it was thought that the viral components accumulated at the ND10 bodies to facilitate viral assembly at late times of infection, but the requirement for PML at early stages of infection indicated that L2 might also direct the viral genome to the ND10 bodies to initiate infection (20, 21). Further studies have examined the replication and transcription of transfected BPV1 DNA in mouse PML null fibroblasts (22), have demonstrated papillomavirus proteins localizing to and interacting with ND10 bodies (23–27), and have shown an increase in the number of PML bodies in keratinocytes and organotypic rafts harboring replicating HPV genomes (22). However, there have been no additional studies that have directly examined the functional role of ND10 bodies in the initiation of HPV infection.

In the present work, we have examined the roles of PML, Sp100, and Daxx in the early stages of HPV18 infection of primary human keratinocytes. Using small interfering RNA (siRNA) technology, we have individually downregulated each protein and examined the effects on HPV18 transcription, replication, and immortalization of keratinocytes. We show that reduction of Sp100 levels results in increased viral transcription, enhanced replication, and increased colony formation in a quantitative immortalization assay. Thus, Sp100 functions as a repressor of viral infection.

RESULTS

Downregulation of ND10 body components in primary HFKs. The cellular proteins Sp100, Daxx, and PML are key components of the ND10 body. To examine the roles of these proteins in the establishment of HPV genomes, each protein was downregulated in primary human foreskin keratinocytes (HFKs). Pools of siRNAs targeting PML, Sp100, or Daxx and a nontargeting control were tested for the ability to downregulate endogenous protein expression. To determine the efficiency and duration of siRNA depletion, protein lysates were harvested at 48, 72, and 96 h after the initial siRNA transfection and analyzed by Western blotting (Fig. 1A and B). Specific depletion of each ND10 component was achieved by 48 h posttransfection and maintained through the 96-h time point. Quantitation of the Western blot assays showed that after 48 h we could achieve approximately 45, 70, and 75% knockdown of PML, Sp100, and Daxx, respectively.

To determine the effect of siRNA depletion of each protein on ND10 body formation, cells were seeded onto coverslips and transfected with pools of PML, Sp100, or Daxx siRNA. After 48 h, cells were fixed and costained for PML and Sp100 or PML and Daxx (Fig. 1C) and imaged by confocal microscopy. The total amount of each protein per cell and the number of ND10 bodies were quantitated by three-dimensional (3D) image processing (Fig. 1D and E). Specific downregulation of the total protein of each ND10 component was observed. Downregulation of Daxx or Sp100 had no effect on the number of bodies and no effect on the localization of the other components to the bodies. However, as noted previously (28), complete downregulation of PML resulted in dissolution of the ND10 bodies (as detected with Sp100 and Daxx antibodies) in approximately one-third of the cells. The remaining PML-deficient cells contained residual Sp100 and Daxx bodies, which contained either very low levels or no detectable PML. The latter bodies had a disorganized appearance compared to the uniformly shaped ND10 bodies observed in untreated cells. Nevertheless, as shown by immunoblot analysis in Fig. 1A and B, the overall levels of Daxx and Sp100 did not change when PML was depleted.

Depletion of ND10 protein Sp100 results in enhanced colony formation in a quantitative HPV18 immortalization assay. Oncogenic HPV types will replicate in and immortalize primary human keratinocytes, and so, to measure the efficiency of establishment of HPV infection, we employed a quantitative immortalization assay (29). When viral DNA is cotransfected with a plasmid encoding a selectable marker (pRSV2neo), only HPV-containing keratinocytes efficiently survive drug selection and form proliferative colonies that survive long-term culture (29). Thus, we used this assay to investigate the roles of the three ND10 components in the establishment of HPV infection.

Cloned HPV18 genomes were cleaved from their vector and religated at low concentrations to facilitate intramolecular recircularization. HFKs were depleted of PML, Sp100, and Daxx as described above and after 48 h electroporated with a 2:1 molar ratio of recircularized HPV18 DNA (or pUC18 DNA) and the pRSV-neo plasmid. Electroporated keratinocytes were plated at several dilutions and selected for 4 days with G418. After 2 to 3 weeks, keratinocyte colonies formed and were counted and graphed (Fig. 2A and B). Cells depleted of PML routinely showed a 3-fold reduction in colony-forming potential (Fig. 2A), consistent with the previously described requirement for PML in BPV1 infection of mouse fibroblasts (20). Conversely, Sp100 siRNA-treated keratinocytes exhibited an approximately 3-fold increase in the number of HPV18-positive colonies (Fig. 2A). Notably, Daxx siRNA treatment had no effect on colony-forming potential. The assay was repeated with at least five different HFK donor strains, and Sp100 siRNA-treated HFKs consistently showed a marked enhancement of colony formation compared to those treated with the control siRNA. Cells depleted of PML consistently formed no colonies or fewer colonies than controls.

In these experiments, keratinocytes were also electroporated with pRSV-neo in the absence of HPV18 DNA as a control. As described previously, this resulted in only a few small colonies that do not proliferate in long-term culture (29). However, as shown in Fig. 2A, an increase in HPV-negative colonies was observed in Sp100-depleted HFKs, though the overall number of colonies was markedly lower than that of Sp100-treated HPV18-dependent colonies. This result indicates that Sp100 is not completely specific for HPV18 and that the absence of Sp100 can result in the increased formation of transient neomycin-resistant colonies.

ND10 proteins have opposing roles in viral transcription. There are several isoforms of the Sp100 protein, some of which contain protein domains known to activate or repress transcription (30). To determine if the enhancement of colony formation observed in the absence of Sp100 was due to Sp100-mediated regulation of viral transcription, we analyzed the levels of two spliced HPV18 messages 4 days after the transfection of viral DNA. Cells were transfected with PML, Daxx, or Sp100 siRNA or a nontargeting control as described above and 2 days later electroporated with recircularized HPV18 DNA. After 96 h, total RNA was harvested and E1^E4 and E6*I transcripts were measured by quanti-

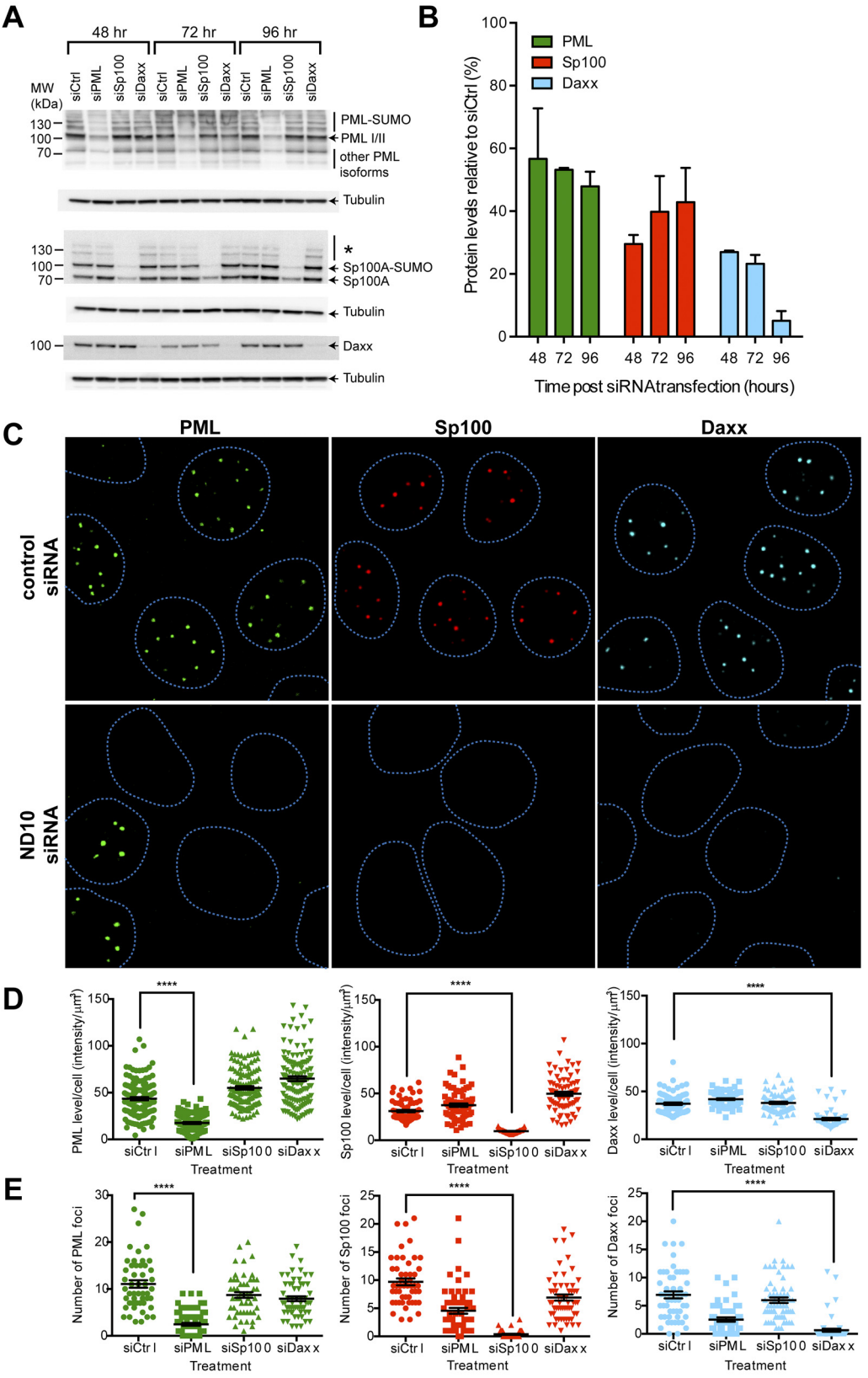

FIG 1. siRNA depletion of ND10-associated proteins in primary human keratinocytes. (A) Immunoblot analysis of ND10 proteins at 48, 72, and 96 h posttransfection of siRNA. Fifteen micrograms of cellular protein was analyzed with anti-PML, -Sp100, or -Daxx specific antibodies. α-Tubulin was used as a loading control. The major PML, Sp100, and Daxx isoforms are indicated. The Sp100 bands indicated by the asterisk likely represent higher-molecular-weight isoforms and/or double-modified Sp100A. siCtrl, control siRNA; siPML, PML siRNA; siSp100, Sp100 siRNA; siDaxx, Daxx siRNA. (B) Quantitation of Western

(Continued)

tative reverse transcription (qRT)-PCR (Fig. 3A). Consistent with the quantitative immortalization assay, the transcription of both E1^E4 and E6*I (Fig. 3B) was reduced by approximately 50% in PML siRNA-treated cells and enhanced 3- to 6-fold in Sp100 siRNA-treated HFKs. While Daxx siRNA treatment did not show an effect on the overall immortalization potential, viral transcription was reduced about 50% at 4 days posttransfection. With the exception of Daxx siRNA treatment, these changes in viral transcription follow the same trend as that observed in the colony formation assay and indicate that PML and Sp100 modulate viral transcription, which may, in turn, determine the efficiency of HPV18-mediated immortalization.

Sp100 depletion enhances HPV DNA replication at early stages of infection. The ND10 components differentially regulated early HPV transcription, and therefore, we questioned whether they would also modulate viral DNA replication. Thus, cells were transfected with siRNAs against PML, Daxx, and Sp100 or a nontargeting control and 2 days later electroporated with recircularized HPV18 DNA. After 96 h, total cellular DNA was isolated and analyzed for viral replication by Southern blot analysis and by quantitative PCR (qPCR). To ensure that viral DNA had replicated in the eukaryotic cells and measured DNA was not transfected input DNA, samples were digested with DpnI, which specifically cleaves DNA methylated in bacteria (31). qPCR primers were designed to amplify a short fragment that spanned two DpnI sites in the E6 gene (Fig. 4A) and therefore will amplify only DpnI-resistant viral DNA. Indeed, viral replication mirrored the results obtained in the transcriptional studies; DNA replication was reduced ~65% in PML siRNA-treated cells and was consistently increased 2- to 4-fold in Sp100 siRNA-treated samples (Fig. 4B). As observed in the immortalization assay, Daxx siRNA treatment consistently reduced viral DNA replication without reaching significance. Viral DNA was also analyzed by Southern analysis; this confirmed the results obtained by qPCR and additionally showed that the replicating viral DNA was full length (Fig. 4C).

Downregulation of Sp100 does not have long-term effects on the viral genome copy number or levels of viral transcription. In the absence of Sp100, viral transcription and replication were enhanced at early time points after the electroporation of HPV18 DNA into HFKs. However, we questioned whether this initial enhanced transcription and replication would be maintained after viral DNA became established. To this end, we isolated individual keratinocyte colonies that grew out from each transient siRNA treatment condition. A total of 52 colonies (15 control siRNA, 6 PML siRNA, 19 Sp100 siRNA, and 12 Daxx siRNA colonies) were expanded and cultured for approximately 4 weeks before total RNA and DNA were prepared from each clone. Although there was variation in the levels of viral DNA (Fig. 5A) and RNA (Fig. 5B) among the clones, there was no consistent increase or decrease in these levels between the groups of clones that had been transiently treated with siRNA prior to electroporation. This indicates that the repressive effects of Sp100 on the viral genome occur only at the early stages of infection as the virus attempts to establish its genome. Downregulation of Sp100 could transiently increase transcription from each viral genome shortly after infection. Alternatively, our data may suggest that depletion of Sp100 could allow a larger number of genomes to efficiently establish infection, giving rise to a larger number of HPV-positive cells, all with similar copy numbers and transcriptional activities.

siRNA depletion of ND10 components has no effect on viral replication or transcription in keratinocytes stably maintaining HPV18 genomes. To further analyze whether ND10 components regulate viral transcription and replication in keratinocytes that contain stably replicating extrachromosomal HPV18, we introduced the same ND10 siRNAs into a cell line containing extrachromosomal HPV18 DNA. The HPV18 cell line expressed each of the ND10 components, and each could be efficiently downregulated by the same siRNA technique used for primary HFKs (Fig. 6A). However, in this case, there was no difference in the levels of E1^E4 and E6*I transcripts (as measured by qRT-PCR) at 3 days posttransfection (Fig. 6B). Likewise, there was no change in the viral DNA copy number after siRNA treatment, as monitored by qPCR for viral DNA at 3 days posttransfection (Fig. 6C). To ensure that the siRNA treatment did not change the extrachromosomal status of the viral genome and to confirm the DNA qPCR results, total DNA was also analyzed by Southern hybridization (Fig. 6D). There was no change in viral genome levels after the siRNA treatments, and the viral genomes were present as supercoiled, extrachromosomal elements. These data, taken together with the failure to see long-term effects on viral transcription and the genome copy number after Sp100 depletion, indicate that Sp100 represses the viral genome only during the initial stages of viral genome establishment.

Sp100 can repress viral transcription in a replication-independent manner. Sp100 could directly repress viral RNA synthesis, or it could repress viral DNA replication, resulting in fewer DNA templates for transcription. To determine whether Sp100 directly represses viral transcription, we generated a replication-incompetent mutant genome containing a stop codon (in the HpaI site located at nucleotide [nt] 2472) in all three reading frames in the E1 gene of HPV18. This mutation truncates the E1 protein at amino acid residue 520 and is designated C-TTL. Wild-type or mutated HPV18 genomes were recircularized and electroporated into primary HFKs as described above, and total DNA and RNA were isolated 48 h later. As expected, replicated (DpnI-resistant) viral DNA was not detectable in cells electroporated with the E1 C-TTL mutant genomes, whereas the wild-type genome replicated efficiently (Fig. 7A and B). When cells were pretreated with the ND10 siRNA, each had a similar effect on

Figure Legend Continued

blot assays for the PML, Sp100, and Daxx proteins depleted at 48, 72, and 96 h. Results are from two independent experiments. Error bars represent the SEM. (C) Primary HFKs cultured on glass coverslips were transfected with 30 nM nontargeting control siRNA or siRNA targeted to PML, hDaxx, or Sp100. Cells were stained at 48 h posttransfection with PML (green), Sp100 (red), or Daxx (cyan) antibodies. Nuclei (outlined with blue dots) were detected by DAPI. Images are single optical slices collected by confocal microscopy. (D) Total PML, Sp100, or Daxx levels per cell were determined with Imaris 3D image quantitation software from at least 75 cells per siRNA treatment. An example representative of three independent experiments is shown. An unpaired Student *t* test was used to determine the statistical significance of the data. Error bars represent the SEM. ****, $P < 0.0001$. (E) The number of ND10 bodies remaining after siRNA treatment was quantitated with ImarisCell. Results were calculated from at least 50 cells collected from three independent experiments. Error bars represent the SEM. ****, $P < 0.0001$.

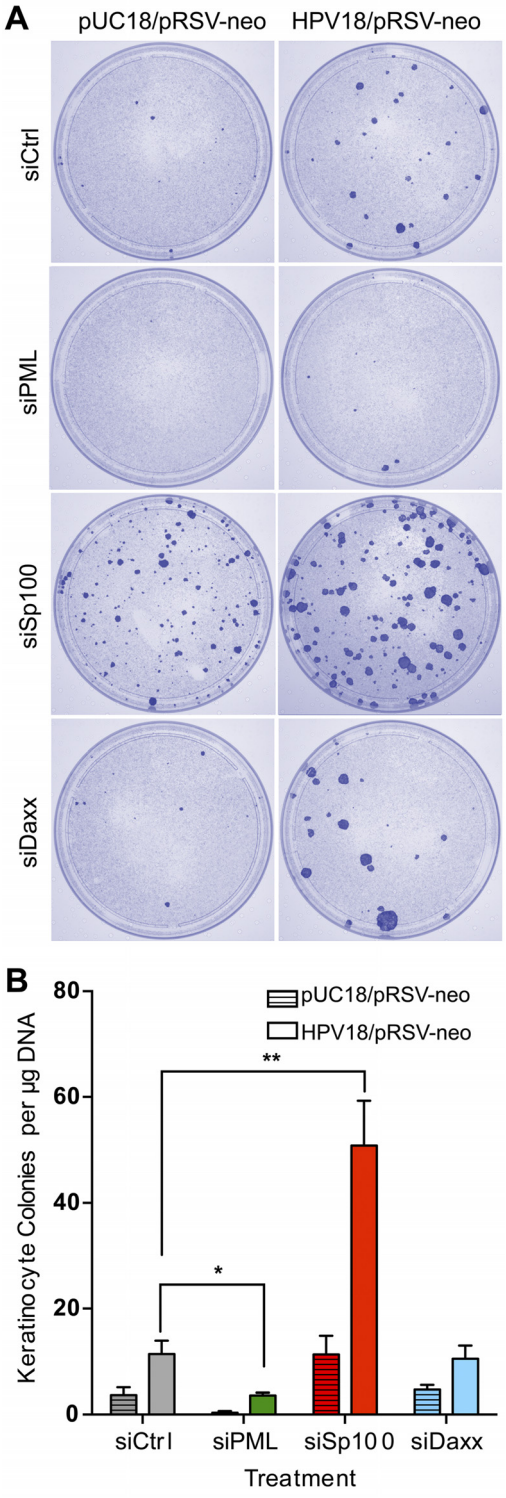

FIG 2 Downregulation of Sp100 results in enhanced HPV18-dependent colony formation. (A) PML, Sp100, and Daxx were depleted by siRNA for 48 h prior to electroporation of recircularized HPV18 DNA and pRSV2neo or pUC18 and pRSV2neo. A total of 5×10^5 electroporated cells were selected for 4 days with 200 μg/ml G418 and cultured for approximately 2 weeks. Keratinocyte colonies were stained with methylene blue. (B) The number of colonies present after each treatment is shown. Results are from four independent experiments with HFKs from five different donors. Paired Student *t* tests were used to determine statistical significance. Error bars represent the SEM. *, $P < 0.05$; **, $P < 0.01$.

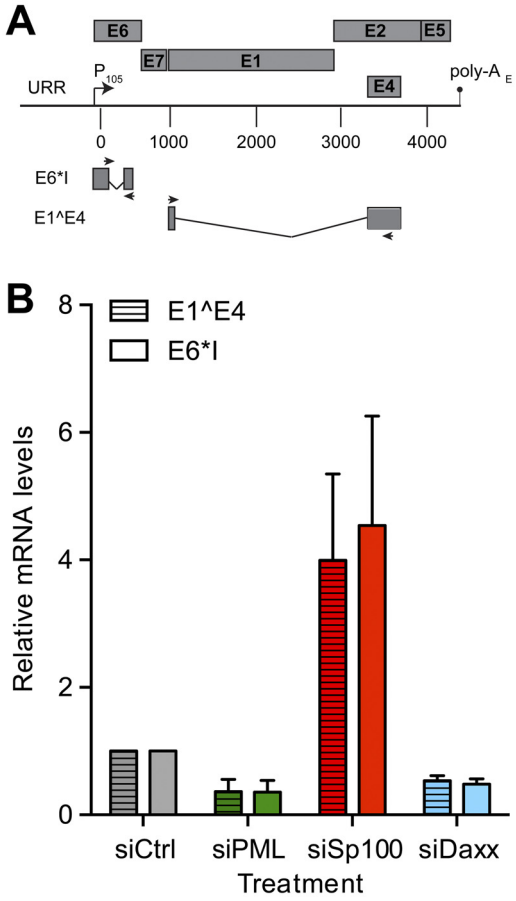

FIG 3 HPV18 transcriptional activity is enhanced when Sp100 is depleted. (A) Diagram of the qRT-PCR strategy used to detect viral spliced mRNA. Primers were designed across exon-exon junctions of two major HPV18 spliced mRNAs, E6*I and E1^E4. The upstream regulatory region (URR), the early promoter (P_{105}), and the early polyadenylation site (poly-A_E) are indicated. Numbering indicates nucleotide positions in the PAVE-HPV18 genome (http://pave.niaid.nih.gov) (52). (B) qRT-PCR was performed in triplicate with 25 ng of reverse-transcribed RNA at 96 h postelectroporation of HPV18 DNA. Values were normalized to glyceraldehyde 3-phosphate dehydrogenase and are shown as fold changes relative to control siRNA. The data are the averages of three independent experiments. Error bars represent the SEM.

wild-type viral genome replication, as shown above (Fig. 4B and C).

Viral RNA from the E1-mutated genomes could be detected, but it was greatly reduced compared to the wild type. Nevertheless, Sp100 depletion increased the levels of viral transcription from the replication-incompetent genome (Fig. 7B and C). Thus, Sp100 can repress viral transcription in the absence of viral replication. Furthermore, the observation that much higher levels of RNA are transcribed from the wild-type genome indicates that much of the observed transcription must be from newly replicated daughter molecules. Since Sp100 depletion results in higher levels of wild-type HPV18 transcription, we can conclude that Sp100 can repress both incoming and nascently replicated viral DNA.

Sp100 depletion enhances transcription and replication of incoming viral particles. The HPV life cycle requires keratinocyte differentiation, and viral particles can only be produced in keratinocytes in an organotypic raft culture system. The studies de-

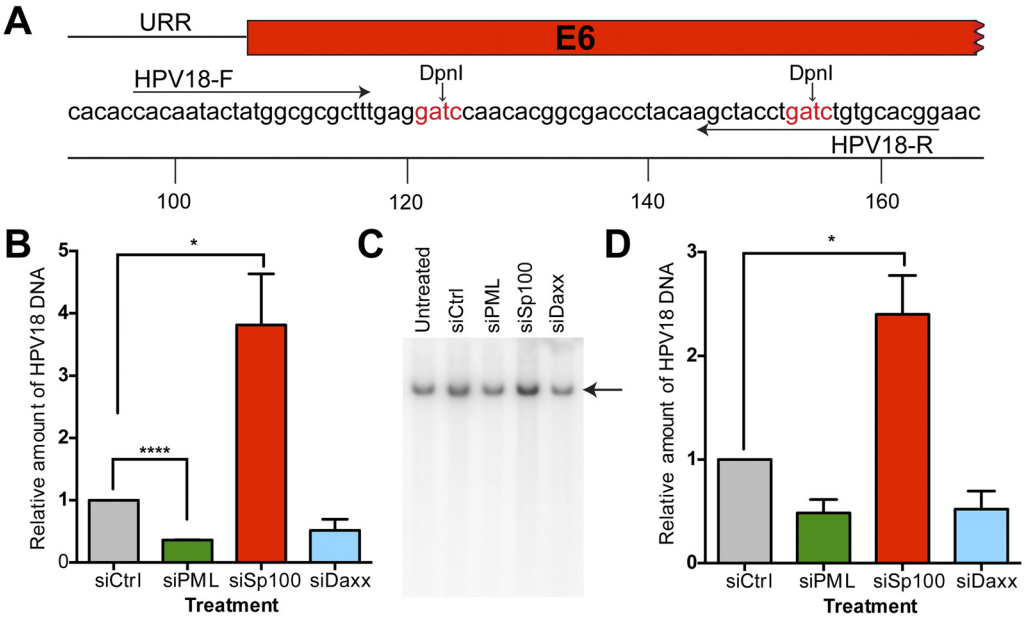

FIG 4 HPV18 replication is increased in the absence of Sp100. (A) qPCR primers and DpnI restriction sites in the HPV18 genome are shown. Nucleotide numbers are from the PAVE-HPV18 genome. The upstream regulatory region (URR) is indicated. (B) DNA qPCR was performed at 96 h postelectroporation of HPV18 DNA into ND10 siRNA-treated HFKs. Prior to analysis, total cellular DNA was digested with NcoI and DpnI to linearize the genome and remove unreplicated input DNA. Values are graphed relative to control siRNA-treated samples. The data are the averages of three independent experiments with three different strains of keratinocytes. The paired Student *t* test was used to determine statistical significance. Error bars represent the SEM. *, $P < 0.05$; ****, $P < 0.0001$. (C) Cellular DNA isolated from ND10 siRNA-treated cells electroporated with HPV18 DNA was digested with NcoI and DpnI and separated by agarose gel electrophoresis. Viral DNA was detected by Southern blot analysis with a ^{32}P-labeled HPV18 DNA probe. The arrow indicates linearized HPV18 DNA. Samples were harvested at 96 h after electroporation. (D) Phosphorimage analysis of Southern blot assays in three independent experiments. The paired Student *t* test was used to determine statistical significance. Error bars represent the SEM. *, $P < 0.05$.

scribed above were conducted with viral DNA because of the difficulties in producing HPV virions for infectivity studies. However, it was important to confirm that Sp100 could repress viral genomes delivered by the natural route of infection. To this end, we produced HPV18 quasivirions by cotransfecting recircularized HPV18 genomes into 293TT cells along with an HPV18 L1/L2 expression vector (pSheLL18). HPV18 virion particles were isolated and purified by OptiPrep gradient centrifugation. Viral particles could efficiently infect primary keratinocytes, as measured by spliced viral mRNA species (E1^E4 and E6*I), which were detectable when cells were infected with 1, 10, or 100 viral genome equivalents (vge)/cell (data not shown).

To test the effect of the ND10 components on the infectivity of HPV18 quasivirus, primary HFKs were again depleted of ND10 components and infected with 100 vge/cell of HPV18 quasivirus at 48 h posttransfection. At 36 and 96 h postinfection, total RNA was collected and analyzed for E1^E4 and E6*I transcript levels. At 36 h postinfection, viral transcription was reduced ~25% in the PML siRNA-treated samples, whereas Sp100-depleted samples showed an ~50% increase in transcription (Fig. 8A and B). Although modest, the decrease in transcription after PML depletion was significant, at least for the E1^E4 transcript. After Sp100 depletion, the increase in the levels of E1^E4 and E6*I transcripts was consistent and statistically significant (Fig. 8A and B).

Additionally, we tested the effect of the ND10 components on HPV18 DNA replication when the viral DNA was delivered by infection. As described above, cells were depleted of the ND10 components and infected with HPV18 at 100 vge/cell. After 96 h postinfection, total DNA was collected and analyzed for viral replication by qPCR. Cells depleted of Sp100 consistently showed an ~2-fold increase in viral replication compared to control siRNA-treated samples (Fig. 8C). These data confirm the results obtained with nucleofection of viral DNA (Fig. 3B and 4) and show that Sp100 can repress both viral transcription and replication from incoming virion particles.

DISCUSSION

In this study, we examined the roles of the PML, Sp100, and Daxx components of the ND10 body in the establishment of HPV infection. Our goal was to analyze the roles of these proteins in a model that was as close as possible to natural infection. Thus, we carried out all of our experiments with primary human keratinocytes and downregulated the endogenous ND10 proteins by transient transfection with siRNA molecules that had been designed to avoid producing off-target effects or inducing the IFN response (32). Viral genomes were introduced into these cells by nucleofection, an electroporation technique that creates a transitory pore in cellular membranes and ensures that small amounts of DNA are delivered directly to the nucleus (33). Viral establishment was quantified by direct readout of viral transcription and replication or by quantifying HPV18-dependent immortalization of keratinocytes. The findings were verified by using viral DNA packaged *in vivo* and delivered to the keratinocyte in an HPV18 virion particle.

Using these methods, we find that, of the three proteins tested, Sp100 has the most notable effects on HPV18 transcription, replication, and keratinocyte immortalization. Downregulation of Sp100 results in an increase in all three readouts of viral infection, suggesting that it is a repressor of HPV18 infection. Our results

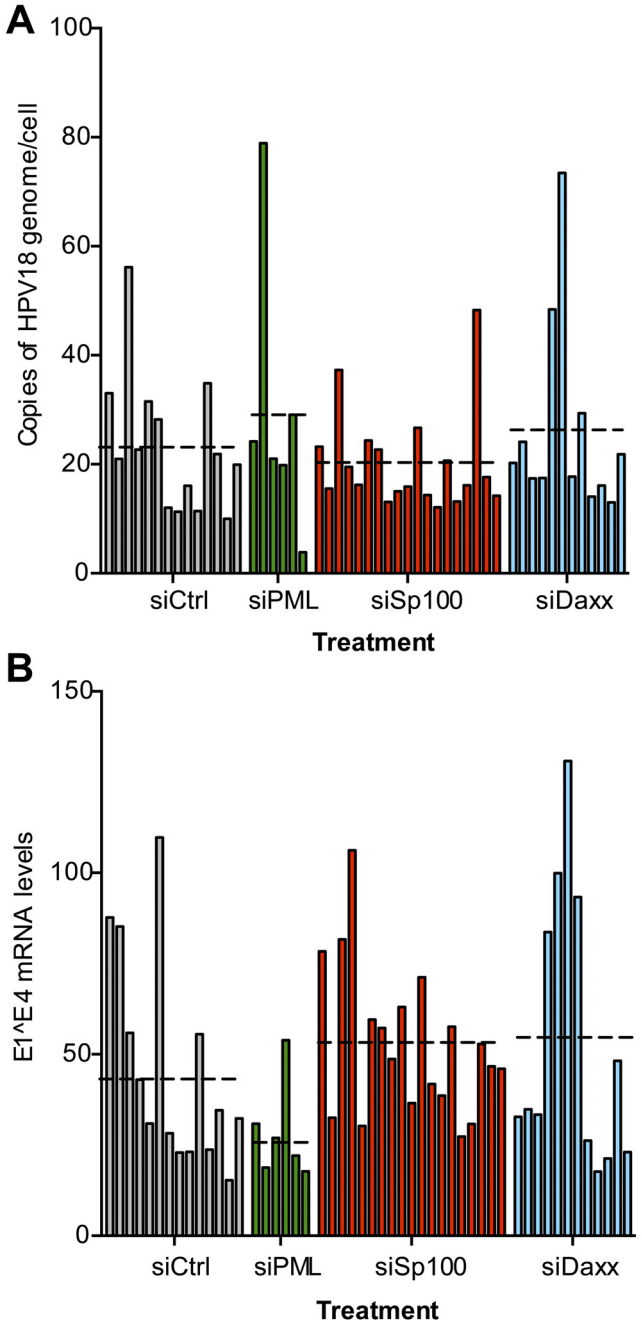

FIG 5 HPV18 transcription and replication are not increased in the long term in cells that underwent an initial depletion of ND10 proteins. (A) qPCR for HPV18 DNA copy number in individual immortalized keratinocyte clones. Colonies were isolated from G418-selected keratinocyte colonies arising after transient siRNA depletion of ND10 proteins and subsequent electroporation of HPV18 DNA. The data presented are numbers of HPV18 genome copies per cell in each clone. Levels of β-actin DNA (a single-copy gene) were used to normalize the HPV18 levels. Colonies were obtained from three independent experiments. Each dashed line represents the average copy number for each siRNA condition. (B) qRT-PCR for E1^E4 transcripts from immortalized clones. cDNA reverse transcribed from 25 ng RNA was analyzed for each keratinocyte clone. Data are E1^E4 mRNA levels normalized to the cellular gene for the TATA box binding protein. Results are from colonies expanded in three independent experiments. Each dashed line represents the average level for each siRNA condition.

show that downregulation of Sp100 results in increased viral transcription at very early times after the entry of viral DNA, and so, repression of replication and immortalization might be due to indirect effects on viral transcription. To further investigate this, we analyzed the effect of Sp100 downregulation on a replication-defective HPV18 genome. Although the transcription of this mutant genome was considerably reduced compared to that of the wild type, Sp100 depletion still resulted in a severalfold increase in viral E6*I and E1^E4 mRNA species. Therefore, Sp100 results in decreased viral transcription even in the absence of viral DNA replication. Depletion of Sp100 could result in increased transcription per viral genome, or else it could allow a larger percentage of genomes to efficiently establish a long-term infection, thus resulting in a larger number of HPV-positive cells. The fact that we observe an increase in HPV18-dependent keratinocyte colonies but no changes in levels of viral replication and transcription within the colonies suggests that Sp100 is modulating viral genome establishment rather than simply increasing viral transcription and replication.

Sp100 has been described as a potent repressor of viral gene expression for several herpesviruses, and all have evolved different mechanisms to counteract this repressive effect. The alphaherpesvirus HSV-1 utilizes ICP0 to induce the degradation of both PML and Sp100 (reviewed in reference 34). HCMV, on the other hand, utilizes both a tegument protein, pp71, and an early gene product, IE1, to induce the loss of SUMO-modified Sp100, leading to its degradation (11), and VZV counteracts ND10 protein sequestration by using an ICP0 homologue, ORF61p (35). Therefore, many DNA viruses are equipped to evade Sp100-mediated intrinsic host defenses.

Sp100 has four primary isoforms, Sp100A, Sp100B, Sp100C, and Sp100HMG (36). All four isoforms have an amino-terminal domain that promotes dimerization and association with heterochromatin protein 1 (7, 36). The shortest and most abundant isoform, Sp100A, contains only these domains and shares almost its entire coding region with the longer isoforms. The Sp100B, Sp100C, and Sp100HMG isoforms contain a SAND domain. In addition, Sp100C contains PHD and bromodomains and Sp100HMG contains an HMG domain. Each of these domains mediates DNA or chromatin binding, which fits well with the proposed role of regulation of HPV transcription. Notably, the Sp100A isoform is targeted for deSUMOylation and degradation by the IE1 and IE2 proteins of HCMV (12) and by ICP0 of HSV (30). Furthermore, a recent study suggested Sp100A as a possible activator of gene transcription through chromatin decondensation at viral promoters (37), suggesting that the different isoforms of Sp100 may play opposing roles with regard to the activation and repression of gene expression. Viruses may exploit the functional ratios of these isoforms to modulate viral transcription.

Sp100 strongly repressed HPV18-dependent colony formation but also reduced the number of small control colonies resulting from the transfection of pRSV2neo. This implies that Sp100-mediated repression might not be specific for viral DNA and Sp100 may be a repressor of "foreign" DNA in general. To test this, we carried out preliminary experiments in which we cotransfected the HPV18 genome with a plasmid containing the β-actin promoter and gene. We found that Sp100 depletion specifically affected HPV transcription but not transcription from the actin promoter (data not shown). Furthermore, Negorev et al. showed that the SAND domain-containing isoforms of Sp100 repress

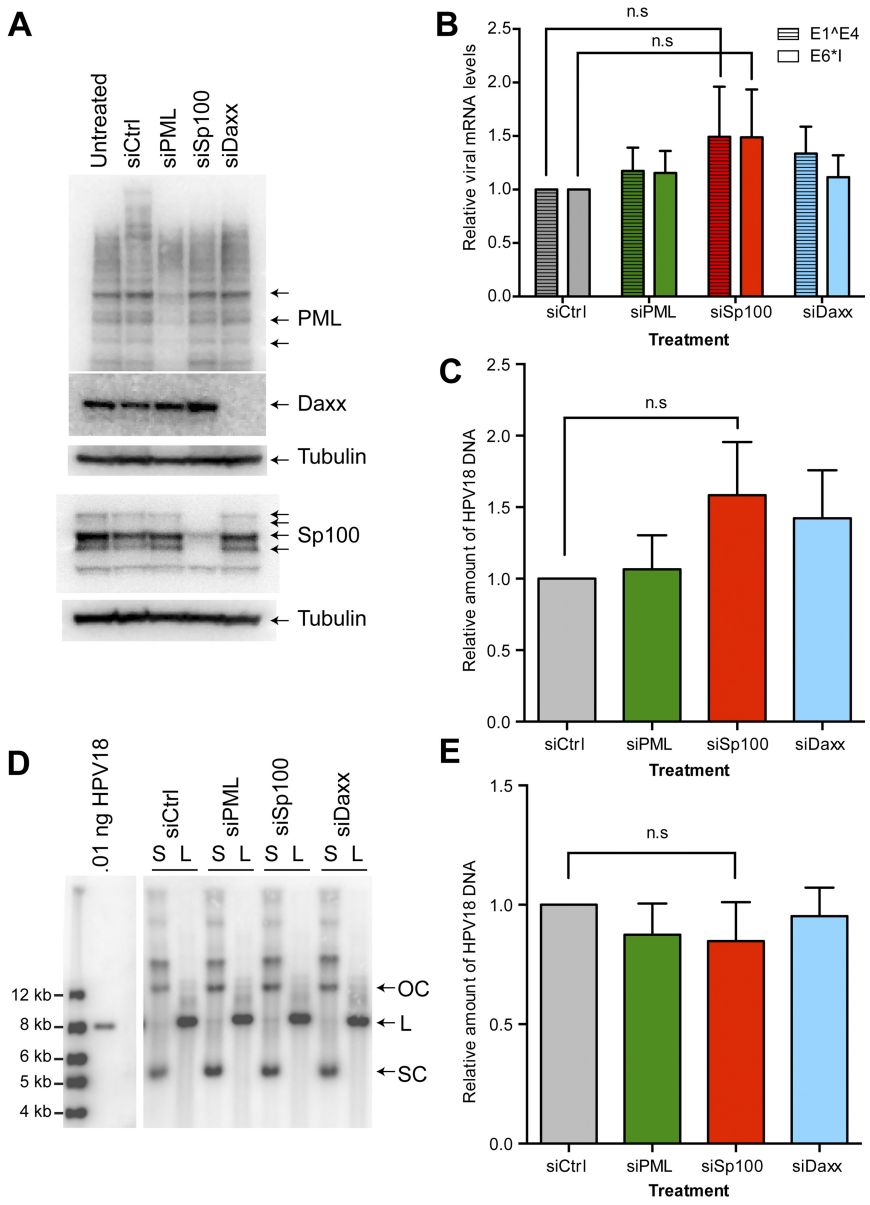

FIG 6 Depletion of ND10 proteins has no effect on the transcription or replication of HPV18 genomes in an established cell line. (A) siRNA depletion of ND10 proteins in an HPV18-harboring cell line, B1. The B1 cell line was transfected with PML, Sp100, or Daxx siRNA or a nontargeting control, and protein lysates were prepared at 3 days posttransfection and analyzed by SDS-PAGE. The levels of PML, Sp100, Daxx, and tubulin were analyzed by Western blotting. (B) DNA qPCR for HPV18 DNA. Fifteen nanograms of total DNA from siRNA-treated B1 cells was analyzed in triplicate by qPCR. The data shown are fold changes in HPV18 DNA relative to control siRNA-treated cells. Error bars represent the SEM of three independent experiments. The paired Student *t* test was used to determine statistical significance. n.s, not statistically significant. (C) qRT-PCR for viral transcription. cDNA from 25 ng of reverse-transcribed RNA was analyzed for HPV18 E1^E4 and E6*I mRNA levels. The data shown are fold changes relative to control siRNA-treated samples. Error bars represent the SEM of three independent experiments. The paired Student *t* test was used to determine statistical significance. n.s, not statistically significant. (D) Southern blot analysis of siRNA-treated HPV18-B1 cell line samples. One microgram of cellular DNA was digested with HindIII for nonlinearized samples (S) or EcoRI to linearize the viral genome (L) and then separated on a 0.8% TAE agarose gel. The open-circle (OC), supercoiled (SC), and linear (L) forms of viral DNA are indicated. A 0.01-ng sample of linear HPV18 was run as a copy number and size control. (E) Phosphorimage quantitation of Southern blot assays. Error bars represent the SEM of three independent experiments. The paired Student *t* test was used to determine statistical significance. n.s, not statistically significant.

promoter (38). These findings are intriguing and suggest that Sp100 specifically represses certain promoters.

The repressive effect of Sp100 was not confined to nucleofection of HPV18 DNA, as viral DNA delivered to cells packaged in histones and in a viral capsid was also repressed by Sp100. However, once viral genomes were established as stably replicating, extrachromosomal plasmids, Sp100 downregulation had no effect on viral transcription and replication. Presumably, viral DNA entering the nucleus has different epigenetic or chromatin marks that can be detected by intrinsic viral defenses, whereas long-term replicating genomes have acquired DNA and chromatin marks that are indistinguishable from host DNA.

Several studies have implicated the minor papillomavirus capsid protein L2 in both delivery of the viral genome to ND10 bodies and rearrangement of the ND10 environment (20, 21, 23, 25, 26). L2 displaces Sp100 and recruits Daxx into the ND10 structure in the human osteosarcoma cell line HuTK$^-$ (23), and we find that L2 also displaces Sp100 from ND10 bodies in human keratinocytes (W.H.S. and A.A.M., unpublished observations). L2 also recruits the HPV transcriptional regulatory protein E2 to ND10 bodies, possibly signifying a role for E2 in modification of the ND10 environment and establishment of HPV transcription (21).

The most notable observation of our study is the repressive effects of Sp100 on HPV18 transcription. However, we also observe that depletion of PML reduces HPV18 transcription, replication, and keratinocyte immortalization. These observations corroborate the findings of Day and colleagues, who demonstrated that BPV1 or pseudovirus is unable to establish an efficient infection in PML-null mouse fibroblasts (20). In agreement, we find that HPV18 transcription (from viral DNA or quasivirus) is decreased in the absence of PML at early times after the infection of primary human keratinocytes. Nakahara and Lambert also analyzed the transcription and replication of electroporated BPV1 DNA in mouse cells lacking PML or expressing a human PML cDNA (22). However, they did not see a significant effect of PML expression on BPV1 genome replication or on E2-dependent transactivation of a thymidine kinase (TK) promoter-driven luciferase plasmid. One difference between our study and

transcription from the respiratory syncytial virus long terminal repeat and the HSV ICP0 promoter but have no effect on the CMV

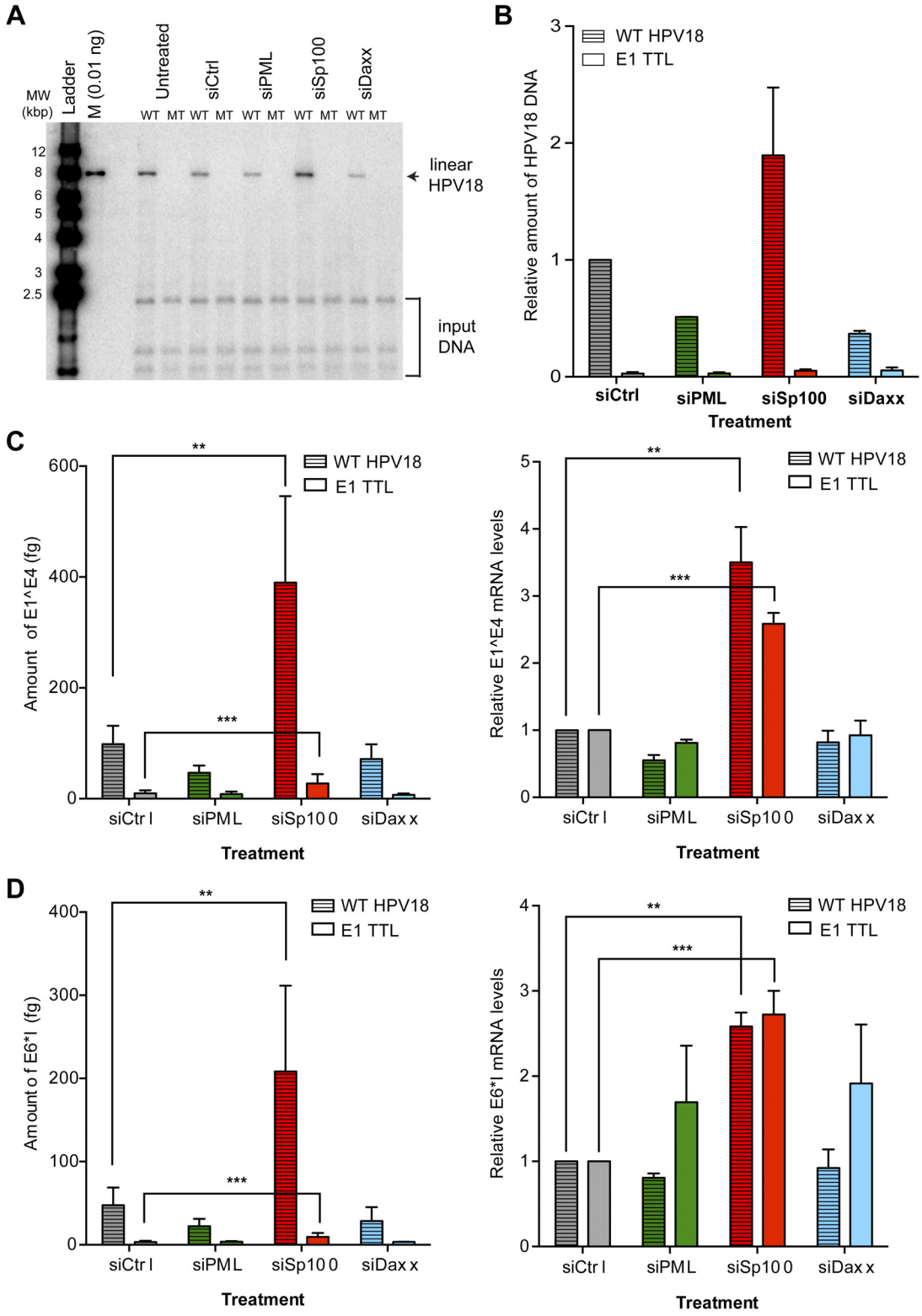

FIG 7 Sp100-mediated repression of HPV18 transcription is not replication dependent. (A) Three micrograms of total DNA from ND10 siRNA-treated cells electroporated with either wild-type HPV18 (WT) or an E1-TTL HPV18 recircularized genome (MT) was digested with NcoI and DpnI and analyzed by Southern blotting. The positions of linear HPV18 DNA and DpnI-sensitive input DNA are indicated. The gel shown is representative of two independent experiments. MW, molecular size. Lane M contained 0.01 ng of HPV18 DNA. (B) Phosphorimage quantitation of Southern blot assay. Results are from two independent experiments. Error bars represent the SEM. (C, D) qRT-PCR assays for E1^E4 (C) and E6*I (D) transcripts were performed with cDNA from 25 ng of reverse-transcribed RNA collected from wild-type and E1-TTL-transfected samples collected at 48 h postelectroporation. The paired Student *t* test was used to demonstrate statistical significance. Results shown are the mean ± SEM of three independent experiments. **, $P < 0.01$; ***, $P < 0.001$.

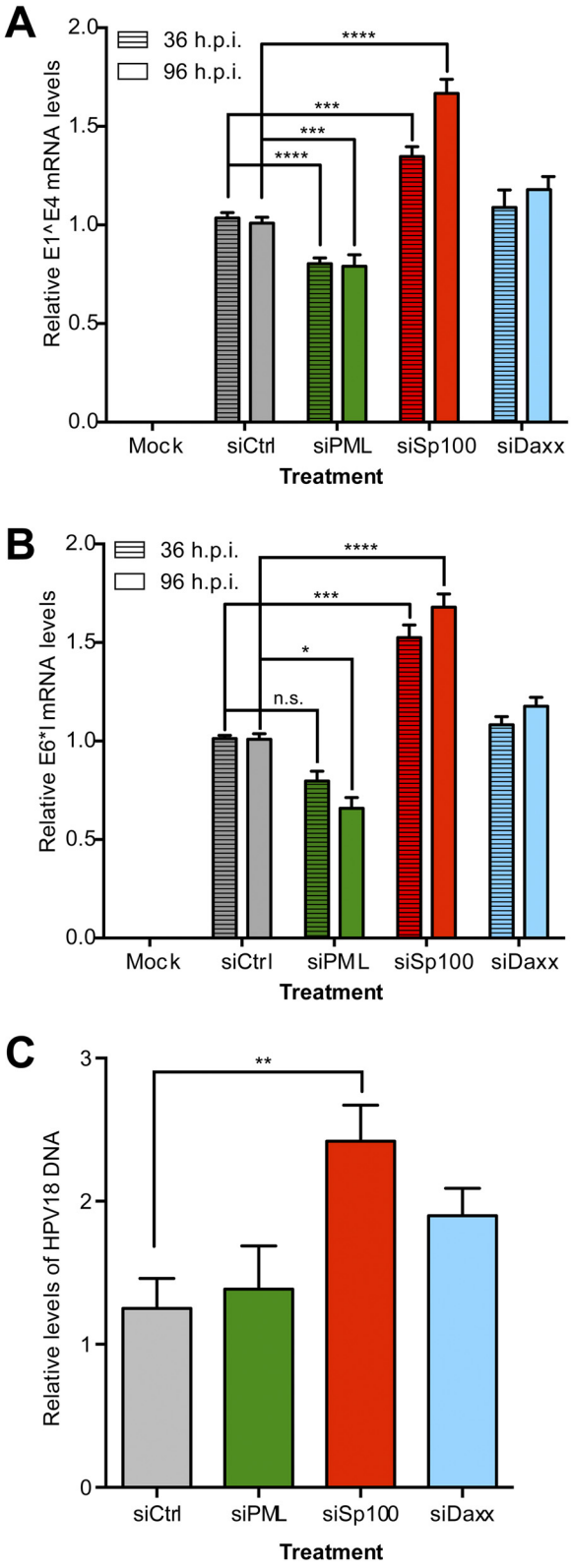

FIG 8 Depletion of Sp100 enhances HPV18 quasivirus infectivity. (A) qRT-PCR analysis of E1^E4 mRNA levels in ND10-depleted, HPV18 quasivirus-infected HFKs. qRT-PCR was performed with cDNA from 25 ng reverse-transcribed RNA. The values displayed are E1^E4 mRNA levels normalized to the cellular gene for the TATA box binding protein. Error bars represent the

(Continued)

that of Nakahara and Lambert is that they used BPV1 genomes cloned into prokaryotic plasmids in their replication assays; cloned genomes have a much lower efficiency of genome establishment than recircularized genomes and sometimes give different phenotypes (39, 40). It is possible that prokaryotic sequences in *cis* to the viral genome could modify the intrinsic immune response to foreign DNA. Nakahara and Lambert analyzed the transcription of a reporter driven by an E2-responsive minimal TK promoter, but as noted above, ND10 proteins can have differential effects on different cellular and viral promoters. Also, those authors concluded that PML might transiently enhance the initial transcription of viral early genes, but not E2-dependent transcription, which presumably occurs after the immediate-early stage of infection. These findings fit well with our finding that ND10 proteins modulate viral transcription and replication only during the very initial stages of viral establishment.

It appears that papillomaviruses are similar to the polyomavirus family members BK virus and simian virus 40, which initiate viral transcription and replication adjacent to ND10 structures but modify the ND10 environment by rearranging or degrading repressive factors like Sp100 to foster the initial amplification of their own genetic programs while not completely destroying the ND10 structure (41, 42). We propose that, while PML is required for efficient initial transcription and replication of HPV, removal of repressive proteins such as Sp100 from the viral genome's initial environment is crucial for successful genome establishment. Displacement of Sp100 by L2 and/or recruitment of E2 to ND10 might be key for efficient viral genome establishment (20, 21, 23). In support of this, nuclear foci generated by expression of the E1 and E2 replication proteins often form adjacent to ND10 bodies (43). The ability of the ND10 components to alter nuclear processes is likely critical for persistent, long-lived HPV infection.

Notably, downregulation of PML resulted in disruption of the ND10 bodies in many cells and dispersal of Daxx and Sp100 into the nucleoplasm or sometimes into non-PML-containing foci containing both proteins. This did not result in an increase in HPV18 transcription that might be expected if Sp100 could only function at ND10 bodies. Thus, Sp100 repression of HPV18 transcription can occur in the absence of ND10 bodies. Negorev et al. have shown that only the A isoform of Sp100 is consistently localized to ND10, while Sp100B, Sp100C, and Sp100HMG isoforms (which repress HSV-1 transcription) are found dispersed throughout the nucleus (30). We predict that the same forms (isoforms Sp100B, Sp100C, and Sp100HMG) will repress HPV establishment. It is possible that the L2 protein directs HPV genomes to PML bodies to avoid the repressive forms of Sp100 found

Figure Legend Continued

SEM of 10 infections in five independent experiments. ***, $P < 0.001$; ****, $P < 0.00001$. (B) qRT-PCR analysis of E6*I mRNA levels in ND10-depleted, HPV18 quasivirus-infected HFKs. qRT-PCR was performed with cDNA from 25 ng reverse-transcribed RNA. The values displayed are E6*I mRNA levels normalized to the cellular gene for the TATA box binding protein. Error bars represent the SEM of 10 infections in five independent experiments. n.s., $P \geq 0.05$; *, $P < 0.05$; ***, $P < 0.001$; ****, $P < 0.0001$. (C) DNA qPCR analysis of HPV18 quasivirus-infected HFKs at 96 h postinfection. DNA PCR was performed with 15 ng of total DNA, and the viral genome quantity was normalized to β-actin. Error bars represent the SEM of six viral infections in three independent experiments. The unpaired Student *t* test was used to determine the statistical significance of the changes. **, $P < 0.01$. WT, wild type; h.p.i., hours postinfection.

throughout the nucleus and disperses small amounts of repressive Sp100 localized to the bodies. Recent studies have provided evidence that the L2-HPV genome complex does not traffic through the nuclear pore upon infection and cells must progress through mitosis to establish infection (44). Notably, ND10 bodies become dispersed during mitosis and only mitotic accumulations of PML protein are present, which do not contain Sp100 (45, 46). Thus, in mitosis, HPV genomes could associate with PML in the absence of Sp100, perhaps enhancing the establishment of infection.

We used infection of keratinocytes with HPV18 quasivirus to corroborate our finding that Sp100 could repress HPV18 transcription. While we did observe a statistically significant increase in viral replication and transcription in Sp100-depleted cells, the effects were more modest than those on electroporated viral DNA. However, these experiments are complicated by the documented ability of minor capsid protein L2 to direct HPV genomes to ND10 bodies while displacing the repressive forms of Sp100 (20, 23, 25). Nevertheless, Sp100 can still repress early viral transcription from quasivirus, showing that the balance between intrinsic cellular defenses and viral countermeasures can be modulated.

Our data identify a direct link between the intrinsic defense system of keratinocytes and the establishment of HPV genomes. A more thorough understanding of how viruses counteract the repressive effects of the intrinsic immune response will provide useful insight into the initial stages of HPV infection.

MATERIALS AND METHODS

Plasmids. Wild-type HPV18 genomes cloned into either pUC18 or pBR322 (47, 48) were cleaved from their prokaryotic vectors with either NcoI or EcoRI, respectively, and recircularized by overnight incubation with T4 DNA ligase at 5 μg/ml DNA. An HPV18 E1 mutant genome was generated by inserting a linker containing stop codons in all open reading frames at nt 2472 (HpaI site) of the viral genome. For qRT-PCR of viral mRNA, cDNA standards were synthesized for HPV18 E1^E4 (nt 914 to 929 and 3434 to 3684) and E6*I (nt 105 to 233 and 416 to 929) and cloned into the EcoRV site of pUC57 (GenScript USA). pRSV-neo was purchased from the American Type Culture Collection (ATCC 37198). pDRIVE-GAPDH was purchased from OpenBiosystems (LIFESEQ95132246), and pCMV-SPORT6-TBP was purchased from OpenBiosystems (MHS6278-202802567). The β-actin plasmid used was purchased from AddGene (AddGene 27123). The pSheLL18 L1/L2 packaging plasmids were provided by Chris Buck (National Cancer Institute; http://home.ccr.cancer.gov/Lco).

Cell culture. Primary human keratinocytes were isolated from neonatal foreskins as described previously (49) and with NIH Institutional Review Board approval. Cells were expanded in Rheinwald-Green F medium (3:1 Ham's F-12/high-glucose Dulbecco's modified Eagle's medium [DMEM], 5% fetal bovine serum [FBS], 0.4 μg/ml hydrocortisone, 8.4 ng/ml cholera toxin, 10 ng/ml epidermal growth factor, 24 μg/ml adenine, 6 μg/ml insulin) on a layer of lethally irradiated J2/3T3 murine fibroblasts. Antibiotics were not used unless otherwise noted. For experiments using G418 selection, HFKs were cultured on G418-resistant J2-3T3 murine fibroblasts generated by transfection with linearized pRSV2-neo and subsequent selection in 500 μg/ml G418. Resistant cells were pooled and expanded for frozen stocks. 293TT cells were provided by Chris Buck (National Cancer Institute) and cultured in DMEM–10% FBS with 200 μg/ml of hygromycin B (Roche). The HPV18 HFK cell line B1 was described previously (50).

siRNA transfections. Keratinocytes were seeded at a density of 10,000/cm^2 onto plates containing 15,000 irradiated J2-3T3 cells/cm^2 and cultured overnight. Pools of siRNA duplexes that target PML (L-006547-00-0010), Sp100 (L-015307-00-0005), or Daxx (L-004420-00-0010) or a nontargeting control (D-001810-10-20) were purchased from Dharmacon (Thermo-Fisher). siRNAs were complexed with DharmaFECT 1 transfection reagent in serum-free DMEM and added to fresh F medium at a final siRNA concentration of 30 nM. Cells were incubated with siRNA for 24 to 96 h before harvesting or further experimentation.

Quantitative immortalization assay. We electroporated 10^6 cells with 2 μg recircularized HPV18 DNA by using an Amaxa Nucleofector on program T-007 and the Primary Human Keratinocyte kit (Lonza). Where used, siRNA-treated cells were collected at 48 h posttransfection and prepared for electroporation. Briefly, cells were pelleted and resuspended in Nucleofection Solution (Lonza) with 2 μg recircularized HPV18 DNA and 1 μg pRSV-neo before electroporation. We plated 5×10^5 electroporated cells onto G418-resistant J2-3T3 murine fibroblasts. After 24 h, electroporated keratinocytes were selected for 4 days in 200 μg/ml G418 (Invitrogen). Selection was discontinued, and cells were cultured in the presence of irradiated J2-3T3 cells for approximately 2 weeks, until distinct keratinocyte colonies were visible. Colonies were either fixed with formalin and stained with methylene blue or individually cloned and expanded for viral DNA copy number or transcript analysis.

RNA extraction and qRT-PCR detection of viral transcripts. Total RNA was isolated with the RNeasy Mini-RNA extraction kit (Qiagen). RT reactions were performed with the Transcriptor First-Strand Synthesis kit (Roche) by using 1 μg of total RNA, 60 μM random hexamers, and 2.5 μM oligo(dT) primers. Real-time qRT-PCR was performed with the ABI Prism 7900HT Sequence Detector (Applied Biosystems) and SYBR green PCR master mix (Roche). Each reaction mixture contained 1× SYBR green master mix, cDNA from 1 μg of RNA, and 0.3 μM each oligonucleotide primer in a total volume of 20 μl. In each run, a 10-fold dilution series (5×10^5 to 5×10^{-2} fg) of pUC57-E1^E4, pUC57-E6*I, pDRIVE-GAPDH, or pDRIVE-TBP was included to generate a standard curve of cycle threshold versus $\log_{10}$ quantity (femtograms). PCR was performed in triplicate at 95°C for 15 min, followed by 40 cycles of denaturation at 95°C for 10 s and annealing and extension at 60°C for 30 s. The specificity of each primer pair was determined by dissociation curve analysis, and single amplicons were confirmed by capillary electrophoresis with DNA1000 LabChips on a Bioanalyzer (Agilent Technologies). For the sequences of the primers used, see Table S1 in the supplemental material.

DNA qPCR for viral genome copy number. Total cellular DNA was isolated from keratinocytes with the DNeasy Blood and Tissue kit (Qiagen) at specific times postelectroporation. A 600-ng DNA sample was digested with the DpnI and NcoI restriction endonucleases. After digestion, 15 ng was analyzed by qPCR using 300 nM primers and SYBR green master mix (Roche). The reaction conditions consisted of a 15-min 95°C activation cycle, 40 cycles of 10 s 95°C denaturation and 30 s 60°C annealing, and elongation. Copy number analysis was completed by comparing the unknown samples to standard curves of linearized HPV18 DNA. The β-actin DNA copy number was used as an endogenous control. For the sequences of the primers used, see Table S1 in the supplemental material.

Southern blot analysis. Total DNA was harvested with the DNeasy Blood and Tissue kit (Qiagen). At least 1 μg total DNA was digested with either a single-cut linearizing enzyme (NcoI) for the HPV18 genome or a noncutter (HindIII) to linearize cellular DNA. For transient DNA replication analysis, samples were also digested with DpnI to remove any unreplicated viral DNA. After digestion, samples were separated on 0.8% Tris-acetate-EDTA (TAE) agarose gels. DNA was visualized with 0.5 mg/ml ethidium bromide and transferred onto nylon membranes with a TurboBlotter downward transfer system (Whatman). Membranes were UV cross-linked, dried, incubated with prehybridization blocking buffer, and then incubated overnight with [^{32}P]dCTP-labeled HPV18 DNA in hybridization buffer (0.75× SSC [1× SSC is 0.15 M NaCl plus 0.015 M sodium citrate], 2% SDS, 5× Denhardt's solution, 0.2 mg/ml sonicated salmon sperm DNA, 25 ng [^{32}P]dCTP-labeled HPV18 DNA). Radiolabeled probe was generated from 50 ng of 2× gel-purified linear HPV18 DNA with the Random Prime DNA labeling kit (Roche). Hybrid-

ized DNA was visualized and quantitated by phosphorimaging on a Typhoon Scanner (GE Bioscience).

Indirect immunofluorescence. Cells were cultured on number 1.5 18-mm glass coverslips and fixed with 4% paraformaldehyde–phosphate-buffered saline (PBS). Fixed cells were permeabilized with 0.1% Triton X-100 (Sigma) in PBS and blocked in 5% (vol/vol) normal donkey serum (Jackson Immunoresearch). The antibodies used were goat anti-PML A-20 (Santa Cruz Biotechnology; 1:50 dilution), rabbit anti-PML HPA008312 (Sigma; 1:50), mouse anti-PML PG-M3 (Santa Cruz Biotechnology; 1:50), rabbit anti-Sp100 HPA016707 (Sigma; 1:50), and rabbit anti-Daxx HPA008736 (Sigma; 1:50). Fluorescent secondary antibodies labeled with Alexa 488, Alexa 564, Alexa 594, or Alexa 647 (Jackson Immunoresearch) were used at a 1:100 dilution. Coverslips were mounted by using ProLong Gold with 4′,6-diamidino-2-phenylindole (DAPI; Molecular Probes). Cells were visualized with a Leica SP5 confocal microscope. Exported images were arranged together as a figure assembled with Adobe Illustrator and minimally processed as a group with Adobe Photoshop.

Western blot analysis and antibodies. Cells were lysed in SDS extraction buffer (50 mM Tris-HCl [pH 6.8], 5% [wt/vol] SDS, 10% [vol/vol] glycerol). Protein concentration was determined with a BCA protein assay kit (Thermo-Pierce), and 15 μg total protein was separated on a 4 to 12% bis-Tris polyacrylamide gel (Invitrogen). Proteins were transferred overnight onto polyvinylidene difluoride membrane (Millipore) and subsequently immunoblotted. The antibodies used were rabbit anti-PML A301-167A-2 (Bethyl Laboratories; 1:1,000 dilution), rabbit anti-Sp100 HPA016707 (Sigma; 1:1,000), rabbit anti-Daxx HPA008736 (Sigma; 1:1,000), and mouse anti-α-tubulin T6199 (Sigma; 1:1,000). Species-appropriate secondary antibodies conjugated to horseradish peroxidase (Pierce) were used at a 1:10,000 dilution and detected with SuperDura Western Detection Reagent (Thermo-Pierce). The chemiluminescent signal was collected with a Kodak Bioimager 6000 (Carestream).

HPV18 preparation. HPV18 "quasivirions" were generated as previously described for HPV16 (51). A 19-μg sample of recircularized HPV18 genome and 19 μg of pSheLL18 L1/L2 packaging plasmids were transfected into 7×10^6 293TT cells with Lipofectamine 2000 (Invitrogen). At 48 h posttransfection, cells were lysed in 0.5% Triton X-100 (Sigma)–0.1% Benzonase (EMD Millipore)–0.1% PlasmidSafe (Epicenter)–25 mM ammonium sulfate (pH 9) and incubated overnight at 37°C to mature virions. Lysates were treated with a high salt concentration and low-speed centrifugation, and virions were purified by ultracentrifugation through a three-step OptiPrep (Sigma) gradient (27, 33, and 39%). Gradients were fractioned into 10 250-μl fractions and screened for HPV18 DNA by qPCR (for the primers used, see Table S1 in the supplemental material) and for L1 capsid protein content by SDS-PAGE. Gels were stained with SYPRO Ruby Red (Invitrogen), and fractions containing both viral genomes and L1 protein were pooled and used as viral stocks.

Viral infections. A total of 1.5×10^5 HFKs were seeded into each well of 12-well dishes containing 1.5×10^5 irradiated J2/3T3 cells/well and allowed to grow overnight. Approximately 12 h after seeding, cells were adsorbed for 1 h at 4°C with 100 vge/cell of recombinant HPV18 quasivirus in regular F medium containing 8 U/ml of recombinant furin (New England Biolabs). After 1 h of absorption, cells were washed to remove unbound virus and cultured at 37°C until harvesting at 36 or 96 h.

Image collection, processing, and analysis. Images were collected with a Leica SP5 confocal laser scanning microscope (Leica Microsystems). Stacks of 10 slices (approximate thickness, 1 μm) were collected, and nuclei were identified and surface rendered by DAPI staining (Imaris v. 7.6.4 image analysis software; Bitplane Scientific Software). Conjoined, apoptotic, and mitotic cells were excluded from the analysis. Each nucleus was analyzed for PML, Sp100, or Daxx signal intensity. The total signal was divided by the nuclear volume and graphed on a per-cell basis. The number of PML, Sp100, or Daxx foci per nucleus was determined with the Imaris Cell Module.

Statistical analysis. Values are reported as means with error bars depicting the standard errors of the means (SEM). *P* values, where shown, were calculated by Prism 6 (GraphPad Software) and either paired or unpaired Student *t* tests, as indicated in the figure legends.

SUPPLEMENTAL MATERIAL

Supplemental material for this article may be found at http://mbio.asm.org/lookup/suppl/doi:10.1128/mBio.00845-13/-/DCSupplemental.

Table S1, DOCX file, 0.1 MB.

ACKNOWLEDGMENTS

We are grateful to Koenraad van Doorslaer, Caleb McKinney, and Moon Kyoo Jang for critical reading of the manuscript.

This work was funded by the Intramural Research Program of the NIAID, NIH.

REFERENCES

1. **zur Hausen H.** 1996. Papillomavirus infections—a major cause of human cancers. Biochim. Biophys. Acta **1288:**F55–F78.
2. **Everett RD, Chelbi-Alix MK.** 2007. PML and PML nuclear bodies: implications in antiviral defence. Biochimie **89:**819–830.
3. **Malmgaard L.** 2004. Induction and regulation of IFNs during viral infections. J. Interferon Cytokine Res. **24:**439–454.
4. **Weidtkamp-Peters S, Lenser T, Negorev D, Gerstner N, Hofmann TG, Schwanitz G, Hoischen C, Maul G, Dittrich P, Hemmerich P.** 2008. Dynamics of component exchange at PML nuclear bodies. J. Cell Sci. **121:**2731–2743.
5. **Guldner HH, Szostecki C, Grötzinger T, Will H.** 1992. IFN enhance expression of Sp100, an autoantigen in primary biliary cirrhosis. J. Immunol. **149:**4067–4073.
6. **Spector DL.** 2001. Nuclear domains. J. Cell Sci. **114:**2891–2893.
7. **Sternsdorf T, Jensen K, Reich B, Will H.** 1999. The nuclear dot protein sp100, characterization of domains necessary for dimerization, subcellular localization, and modification by small ubiquitin-like modifiers. J. Biol. Chem. **274:**12555–12566.
8. **Nefkens I, Negorev DG, Ishov AM, Michaelson JS, Yeh ET, Tanguay RM, Müller WE, Maul GG.** 2003. Heat shock and CD2+ exposure regulate PML and Daxx release from ND10 by independent mechanisms that modify the induction of heat-shock proteins 70 and 25 differently. J. Cell Sci. **116:**513–524.
9. **Bernardi R, Pandolfi PP.** 2007. Structure, dynamics and functions of promyelocytic leukaemia nuclear bodies. Nat. Rev. Mol. Cell Biol. **8:**1006–1016.
10. **Everett RD, Freemont P, Saitoh H, Dasso M, Orr A, Kathoria M, Parkinson J.** 1998. The disruption of ND10 during herpes simplex virus infection correlates with the Vmw110- and proteasome-dependent loss of several PML isoforms. J. Virol. **72:**6581–6591.
11. **Kim YE, Lee JH, Kim ET, Shin HJ, Gu SY, Seol HS, Ling PD, Lee CH, Ahn JH.** 2011. Human cytomegalovirus infection causes degradation of Sp100 proteins that suppress viral gene expression. J. Virol. **85:**11928–11937.
12. **Tavalai N, Adler M, Scherer M, Riedl Y, Stamminger T.** 2011. Evidence for a dual antiviral role of the major nuclear domain 10 component Sp100 during the immediate-early and late phases of the human cytomegalovirus replication cycle. J. Virol. **85:**9447–9458.
13. **Maul GG, Negorev D.** 2008. Differences between mouse and human cytomegalovirus interactions with their respective hosts at immediate early times of the replication cycle. Med. Microbiol. Immunol. **197:**241–249.
14. **Cantrell SR, Bresnahan WA.** 2006. Human cytomegalovirus (HCMV) UL82 gene product (pp71) relieves hDaxx-mediated repression of HCMV replication. J. Virol. **80:**6188–6191.
15. **Tavalai N, Papior P, Rechter S, Stamminger T.** 2008. Nuclear domain 10 components promyelocytic leukemia protein and hDaxx independently contribute to an intrinsic antiviral defense against human cytomegalovirus infection. J. Virol. **82:**126–137.
16. **Glass M, Everett RD.** 2013. Components of promyelocytic leukemia nuclear bodies (ND10) act cooperatively to repress herpesvirus infection. J. Virol. **87:**2174–2185.
17. **Kyratsous CA, Silverstein SJ.** 2009. Components of nuclear domain 10 bodies regulate varicella-zoster virus replication. J. Virol. **83:**4262–4274.
18. **Tavalai N, Papior P, Rechter S, Leis M, Stamminger T.** 2006. Evidence

for a role of the cellular ND10 protein PML in mediating intrinsic immunity against human cytomegalovirus infections. J. Virol. **80:**8006–8018.
19. **Schreiner S, Wimmer P, Sirma H, Everett RD, Blanchette P, Groitl P, Dobner T.** 2010. Proteasome-dependent degradation of Daxx by the viral E1B-55K protein in human adenovirus-infected cells. J. Virol. **84:**7029–7038.
20. **Day PM, Baker CC, Lowy DR, Schiller JT.** 2004. Establishment of papillomavirus infection is enhanced by promyelocytic leukemia protein (PML) expression. Proc. Natl. Acad. Sci. U. S. A. **101:**14252–14257.
21. **Day PM, Roden RB, Lowy DR, Schiller JT.** 1998. The papillomavirus minor capsid protein, L2, induces localization of the major capsid protein, L1, and the viral transcription/replication protein, E2, to PML oncogenic domains. J. Virol. **72:**142–150.
22. **Nakahara T, Lambert PF.** 2007. Induction of promyelocytic leukemia (PML) oncogenic domains (PODs) by papillomavirus. Virology **366:**316–329.
23. **Florin L, Schäfer F, Sotlar K, Streeck RE, Sapp M.** 2002. Reorganization of nuclear domain 10 induced by papillomavirus capsid protein L2. Virology **295:**97–107.
24. **Karanam B, Peng S, Li T, Buck C, Day PM, Roden RB.** 2010. Papillomavirus infection requires gamma secretase. J. Virol. **84:**10661–10670.
25. **Florin L, Sapp C, Streeck RE, Sapp M.** 2002. Assembly and translocation of papillomavirus capsid proteins. J. Virol. **76:**10009–10014.
26. **Becker KA, Florin L, Sapp C, Sapp M.** 2003. Dissection of human papillomavirus type 33 L2 domains involved in nuclear domains (ND) 10 homing and reorganization. Virology **314:**161–167.
27. **Becker KA, Florin L, Sapp C, Maul GG, Sapp M.** 2004. Nuclear localization but not PML protein is required for incorporation of the papillomavirus minor capsid protein L2 into virus-like particles. J. Virol. **78:**1121–1128.
28. **Ishov AM, Sotnikov AG, Negorev D, Vladimirova OV, Neff N, Kamitani T, Yeh ET, Strauss JF III, Maul GG.** 1999. PML is critical for ND10 formation and recruits the PML-interacting protein daxx to this nuclear structure when modified by SUMO-1. J. Cell Biol. **147:**221–234.
29. **Lace MJ, Anson JR, Klingelhutz AJ, Lee JH, Bossler AD, Haugen TH, Turek LP.** 2009. Human papillomavirus (HPV) type 18 induces extended growth in primary human cervical, tonsillar, or foreskin keratinocytes more effectively than other high-risk mucosal HPVs. J. Virol. **83:**11784–11794.
30. **Negorev DG, Vladimirova OV, Ivanov A, Rauscher F III, Maul GG.** 2006. Differential role of Sp100 isoforms in interferon-mediated repression of herpes simplex virus type 1 immediate-early protein expression. J. Virol. **80:**8019–8029.
31. **Lacks SA.** 1980. Purification and properties of the complementary endonucleases DpnI and DpnII. Methods Enzymol. **65:**138–146.
32. **Reynolds A, Anderson EM, Vermeulen A, Fedorov Y, Robinson K, Leake D, Karpilow J, Marshall WS, Khvorova A.** 2006. Induction of the interferon response by siRNA is cell type–and duplex length–dependent. RNA **12:**988–993.
33. **Distler JH, Jüngel A, Kurowska-Stolarska M, Michel BA, Gay RE, Gay S, Distler O.** 2005. Nucleofection: a new, highly efficient transfection method for primary human keratinocytes. Exp. Dermatol. **14:**315–320.
34. **Boutell C, Everett RD.** 2013. Regulation of alphaherpesvirus infections by the ICP0 family of proteins. J. Gen. Virol. **94:**465–481.
35. **Walters MS, Kyratsous CA, Silverstein SJ.** 2010. The RING finger domain of varicella-zoster virus ORF61p has E3 ubiquitin ligase activity that is essential for efficient autoubiquitination and dispersion of Sp100-containing nuclear bodies. J. Virol. **84:**6861–6865.
36. **Seeler JS, Marchio A, Sitterlin D, Transy C, Dejean A.** 1998. Interaction of SP100 with HP1 proteins: a link between the promyelocytic leukemia-associated nuclear bodies and the chromatin compartment. Proc. Natl. Acad. Sci. U. S. A. **95:**7316–7321.
37. **Newhart A, Negorev DG, Rafalska-Metcalf IU, Yang T, Maul GG, Janicki SM.** 2013. Sp100A promotes chromatin decondensation at a cytomegalovirus-promoter-regulated transcription site. Mol. Biol. Cell **24:**1454–1468.
38. **Negorev DG, Vladimirova OV, Maul GG.** 2009. Differential functions of interferon-upregulated Sp100 isoforms: herpes simplex virus type 1 promoter-based immediate-early gene suppression and PML protection from ICP0-mediated degradation. J. Virol. **83:**5168–5180.
39. **Howley PM, Schenborn ET, Lund E, Byrne JC, Dahlberg JE.** 1985. The bovine papillomavirus distal "enhancer" is not cis essential for transformation or for plasmid maintenance. Mol. Cell. Biol. **5:**3310–3315.
40. **McBride AA, Howley PM.** 1991. Bovine papillomavirus with a mutation in the E2 serine 301 phosphorylation site replicates at a high copy number. J. Virol. **65:**6528–6534.
41. **Jiang M, Entezami P, Gamez M, Stamminger T, Imperiale MJ.** 2011. Functional reorganization of promyelocytic leukemia nuclear bodies during BK virus infection. mBio **2**(1):e00281-11. doi:10.1128/mBio.00281-11.
42. **Ishov AM, Maul GG.** 1996. The periphery of nuclear domain 10 (ND10) as site of DNA virus deposition. J. Cell Biol. **134:**815–826.
43. **Swindle CS, Zou N, Van Tine BA, Shaw GM, Engler JA, Chow LT.** 1999. Human papillomavirus DNA replication compartments in a transient DNA replication system. J. Virol. **73:**1001–1009.
44. **Pyeon D, Pearce SM, Lank SM, Ahlquist P, Lambert PF.** 2009. Establishment of human papillomavirus infection requires cell cycle progression. PLoS Pathog. **5:**e1000318. doi:10.1371/journal.ppat.1000318.
45. **Everett RD, Lomonte P, Sternsdorf T, van Driel R, Orr A.** 1999. Cell cycle regulation of PML modification and ND10 composition. J. Cell Sci. **112:**4581–4588.
46. **Dellaire G, Eskiw CH, Dehghani H, Ching RW, Bazett-Jones DP.** 2006. Mitotic accumulations of PML protein contribute to the re-establishment of PML nuclear bodies in G_1. J. Cell Sci. **119:**1034–1042.
47. **Cole ST, Danos O.** 1987. Nucleotide sequence and comparative analysis of the human papillomavirus type 18 genome. Phylogeny of papillomaviruses repeated structure E6 and E7 gene products. J. Mol. Biol. **193:**599–608.
48. **Romanczuk H, Howley PM.** 1992. Disruption of either the E1 or the E2 regulatory gene of human papillomavirus type 16 increases viral immortalization capacity. Proc. Natl. Acad. Sci. U. S. A. **89:**3159–3163.
49. **Chapman S, Liu X, Meyers C, Schlegel R, McBride AA.** 2010. Human keratinocytes are efficiently immortalized by a Rho kinase inhibitor. J. Clin. Invest. **120:**2619–2626.
50. **Sakakibara N, Chen D, Jang MK, Kang DW, Luecke HF, Wu S-Y, Chiang C-M, McBride AA.** Brd4 is displaced from HPV replication factories as they expand and amplify viral DNA. PLoS Pathog. doi:10.1371/journal.ppat.1003777.
51. **Pyeon D, Lambert PF, Ahlquist P.** 2005. Production of infectious human papillomavirus independently of viral replication and epithelial cell differentiation. Proc. Natl. Acad. Sci. U. S. A. **102:**9311–9316.
52. **Van Doorslaer K, Tan Q, Xirasagar S, Bandaru S, Gopalan V, Mohamoud Y, Huyen Y, McBride AA.** 2013. The papillomavirus Episteme: a central resource for papillomavirus sequence data and analysis. Nucleic Acids Res. **41:**D571–D578.